

# Flexible Quasi-Three-Dimensional Terahertz Electric Metamaterials

Abul K. Azad,<sup>1\*</sup> Hou-Tong Chen,<sup>1</sup> Xinchao Lu,<sup>2</sup> Jianqiang Gu,<sup>2</sup> Nina R. Weisse-Bernstein,<sup>3</sup> Elshan Akhadov,<sup>1</sup> Antoinette J. Taylor,<sup>1</sup> Weili Zhang,<sup>2</sup> and John F. O'Hara<sup>1</sup>  
<sup>1</sup>MPA-CINT, Los Alamos National Laboratory, P. O. Box 1663, MS K771, Los Alamos, New Mexico 87545, USA  
<sup>2</sup>School of Electrical and Computer Engineering, Oklahoma State University, Stillwater, OK 74078, USA  
<sup>3</sup>ISR-2, Space and Remote Sensing, Los Alamos National Laboratory, P. O. Box 1663, MS B244, Los Alamos, NM 87545, USA  
\*Email: aazad@lanl.gov

**Abstract:** We fabricate quasi-three-dimensional terahertz electric metamaterials by stacking multiple single-layer planar metamaterials fabricated on thin, flexible polyimide substrates. Terahertz time-domain spectroscopy is used to characterize their transmission properties, with which we obtain the frequency dependent complex effective dielectric functions. Increasing the number of layers reduces the resonant transmission minimum, while the extracted effective dielectric functions are independent on the number of layers. The results reveal that the real portions of the dielectric functions only show positive values, however, decreasing the thickness of the polyimide substrates, and thereby the spacing between the adjacent split-ring resonator layers, enables negative electric response.

**Keywords:** Terahertz, Metamaterials, Effective dielectric functions, Quasi-three-dimensional, Polyimide.

doi: 10.11906/TST.015-022.2009.03.02

## 1. Introduction

Electromagnetic metamaterials have enabled numerous exotic electromagnetic phenomena that are difficult to achieve or not available using natural materials, such as negative refractive index [1, 2], perfect lensing [3, 4], and cloaking [5]. They typically consist of sub-wavelength metallic resonators arrays fabricated on dielectric or semiconducting substrates, which collectively respond to either or both the magnetic and electric components of the incident electromagnetic field. By proper scaling, metamaterials have been demonstrated from radio to near visible frequencies. In the past few years, metamaterials research has sparked special interest in the terahertz (THz) community. Planar split-ring resonator (SRR) arrays fabricated on various semiconductor and insulator substrates have proven capable of responding to THz radiation electrically [6, 7] and/or magnetically [8, 9]. The resonant electromagnetic response of metamaterials are an optimistic approach to overcome the limitations of natural materials in the construction of many functional THz devices, some of which have recently been demonstrated using hybrid planar metamaterials [10-13].

However, using the typical metamaterial building blocks such as metallic SRRs [14] and wires [15], there are considerable fabrication challenges in three-dimensional (3D) metamaterials, particular at higher frequencies ( $\geq 100$  GHz). That is, at THz frequencies and above, most metamaterial research has focused on planar (or 2D) structures, though in many respects 3D metamaterials are highly desirable. In order to create 3D metamaterials operating at higher frequencies, one approach is to stack resonator arrays grown on thin substrates [16, 17]. Alternatively, they can be monolithically grown on a substrate using multi-layer processing

[18-21]. The latter process is particularly suitable for optical metamaterials where the spacing between layers is only in the sub-micron or micron range. In principle, either approach is applicable at THz frequencies, though fabrication is not trivial. An additional challenge, at all frequencies, is to create flexible or conformable metamaterials, which would be particularly useful in certain applications, such as electromagnetic cloaking or shielding. Some progress has been made here with multi-layer metamaterials demonstrated in the far-infrared frequency regime by using polyimide [18, 19] or BCB-based polymer [21] fillers between resonator layers.

In this work, we address the issues of flexibility, 3D fabrication, and material parameter extraction of THz metamaterials comprised of metallic electric split-ring resonators (eSRRs) on conformable polyimide (Kapton) substrates. Their transmission properties were characterized using terahertz time-domain spectroscopy (THz-TDS). These are studied as a single-layer and also as quasi-3D metamaterials by stacking up to four layers. In all cases, the measured transmission exhibits a clear minimum at 1.12 THz due to the excitation of the inductive-capacitive (LC) resonance of the eSRR arrays. It evolves into a full band-stop transmission centered at the resonance frequency as the number of layers increases. We find that the substrate thickness, i.e., the spacing between eSRR layers, significantly affects the effective dielectric functions but that the corresponding extracted frequency-dependent complex effective dielectric functions are largely independent of the number of layers.

## 2. Experiments and Analysis

The eSRR structure employed in this work is shown in Fig. 1. The square side length  $A = 40 \mu\text{m}$ , line width  $d = 3 \mu\text{m}$ , capacitor plate length  $l = 12 \mu\text{m}$ , and gap  $g = 3 \mu\text{m}$ . It was patterned to form a planar square lattice of period  $P = 54 \mu\text{m}$  using standard lift-off photolithography methods on a commercially available polyimide film with a measured thickness of  $84 \pm 2 \mu\text{m}$ . Polyimide has been widely used for photonic and electronic devices because of its high electrical and thermal stability [22]. Its flexibility, durability, relatively low refractive index ( $n \cong 2$ ) and absorption ( $\alpha \cong 20 \text{ cm}^{-1}$ ) also make it favorable as a THz metamaterial substrate. During photolithography a regular silicon wafer was attached to the polyimide film to provide mechanical support. Metalization consists of 10 nm of titanium followed by 200 nm of gold. The polyimide-based single layer metamaterials were then cut, visually aligned, and tightly stacked to form the quasi-3D media. All samples had a  $10 \text{ mm} \times 10 \text{ mm}$  active area.

THz transmission measurements were performed with normal incidence to the eSRR plane in a confocal, photoconductive antenna based THz-TDS system [23]. The system generates broadband impulsive THz radiation with a frequency independent beam waist of 3 mm diameter at the sample. The THz electric field was polarized along the gap bearing arm of the eSRRs, as shown in Fig. 1. In all measurements, samples were sandwiched between two 1 mm thick quartz plates. After transmitting through the samples or a reference (two quartz plates in contact with each other), the impulsive THz electric field was coherently recorded in the time-domain. Quartz has an index roughly equivalent to polyimide, which ensures that the front metamaterial layer has similar boundary conditions as subsequent layers. Through Fourier transformation, the complex

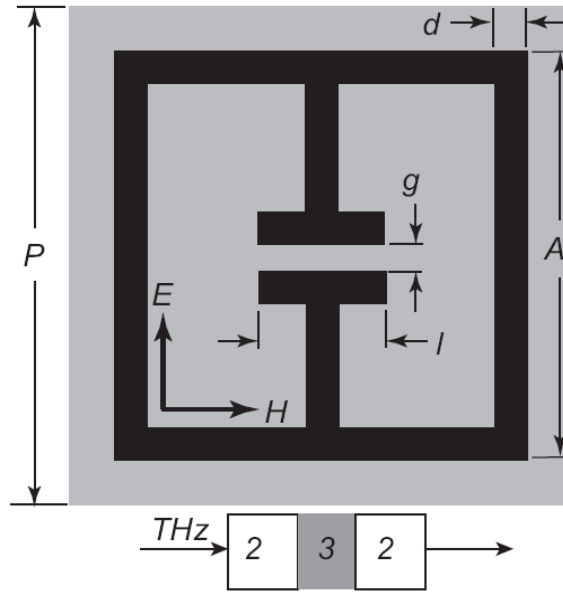


Fig. 1 Diagram of electric split-ring resonator unit cell. Black area represents the metalized resonator and gray area represents the unit cell. E and H show the orientations of incident THz electric and magnetic fields. Bottom shows the schematic of the THz propagation through the metamaterial (region 3) sandwiched between two quartz plates (region 2).

spectra of samples  $E_s(\omega)$  were divided by the reference spectrum  $E_R(\omega)$ , i.e.,  $t(\omega) = E_s(\omega)/E_R(\omega)$ , which simultaneously provides the transmission amplitude and phase information. The effective material parameters of the sample can then be extracted via [24],

$$t(\omega) = t_{23}t_{32} \frac{\exp(ik_0d(\tilde{n}-1))}{1 + r_{23}r_{32} \exp(i2k_0d\tilde{n})}, \quad (1)$$

where  $t_{23}$ ,  $t_{32}$  and  $r_{23}$ ,  $r_{32}$  are the frequency-dependent complex transmission and reflection coefficients at the quartz-metamaterial interfaces;  $k_0$  is the free-space wavenumber,  $d$  is the sample thickness, and  $\tilde{n} = n + ik$  is the sample complex refractive index. Time-windowing allows us to disregard multiple reflections in the quartz plates. Due to the small size and tight transverse packing of the eSRR structures compared to their resonant wavelength, the samples can be considered effectively homogeneous in the two directions transverse to wave propagation [25].

### 3. Results and Discussions

Fig. 2(a) and (b) show the measured THz amplitude and phase following transmission through the metamaterials. The transmission spectra reveal resonances at 1.12 THz due to the inductive-capacitive (LC) response of the eSRRs. With increasing number of layers, the minimum of transmission amplitude decreases and the phase change increases. The four-layer

sample becomes completely opaque at the resonance frequency whereas the single layer transmission minimum is 33%. The low frequency off-resonance transmission amplitude also decreases from 95% in the single-layer metamaterial to 85% in the four-layer metamaterial. The overall linewidth of the LC resonance increases with the number of layers, while there is no significant shift of the center of resonance frequency. We also note the ripple features, most noticeable near and above the LC (1.12 THz) resonance. This is mainly a result of the multiple reflections between the two quartz-metamaterial interfaces. We also notice that the phase slope at off-resonance frequencies and magnitude of the resonant phase perturbation both increase with increasing number of layers.

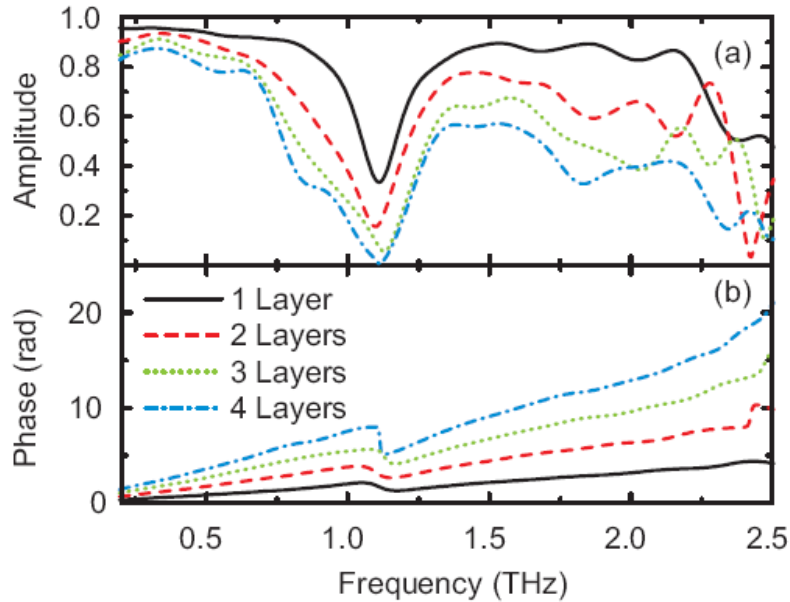


Fig. 2 (a) Measured transmission amplitude of THz electric field through metamaterial samples with different number of layers. (b) The corresponding phase change. The measurements of 1-layer, 2-layer, 3-layer, and 4-layer metamaterials are represented by solid (black), dashed (red), dotted (green), and dashed-dot (blue) curves, respectively.

The amplitude and phase information can be used to extract the metamaterial optical properties, here the frequency dependent complex effective dielectric functions. Note that in a single layer planar metamaterial fabricated on a thick substrate, this will be critically dependent on the definition of the effective metamaterial thickness; this is typically defined assuming a cubic unit cell [26], though there is in fact no clear boundary. In our case, on the other hand, the effective thickness is naturally defined as the physical thickness of the sample, i.e.,  $N \times 84 \mu\text{m}$ , where  $N$  is the number of layers. The complex dielectric functions are then computed from the measured complex indices by  $\varepsilon(\omega) = \varepsilon_r(\omega) + i\varepsilon_i(\omega) = \tilde{n}^2$ . Figs. 3(a) and (b) show  $\varepsilon_r$  and  $\varepsilon_i$ , respectively, for the single- and multi-layer metamaterials, as well as the plain polyimide substrate. The polyimide properties are fairly constant over our frequency range, and at off-resonance frequencies the dielectric functions of metamaterials are very close to those of the polyimide substrate. Additionally, the metamaterial dielectric functions are largely independent of the number of layers, in all cases showing a Lorentzian-like resonance dispersion; this is expected

since an effective medium's dielectric function should not depend on the medium thickness.

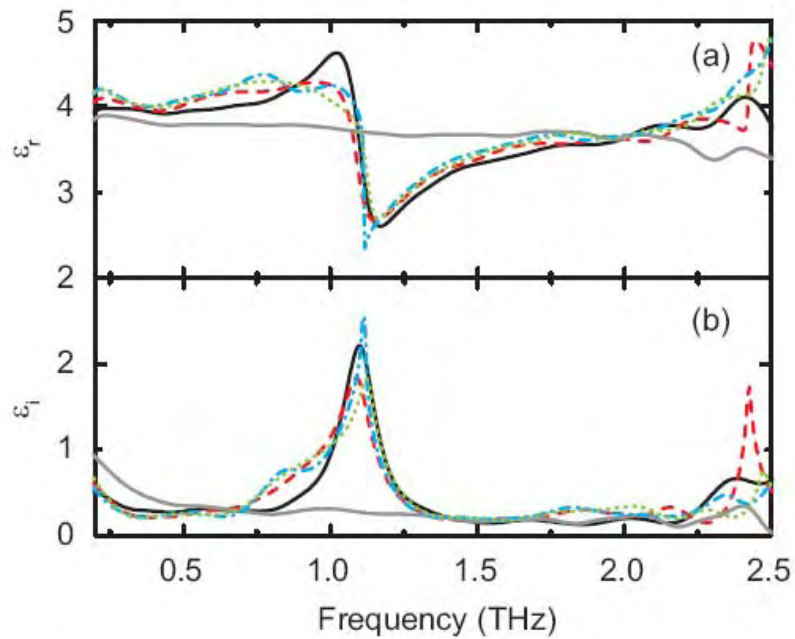


Fig. 3 Extracted (a) real and (b) imaginary effective dielectric functions of the metamaterials. They are presented using the same patterns (colors) as in Fig. 2. The solid gray curve represents the dielectric function of the bare polyimide film.

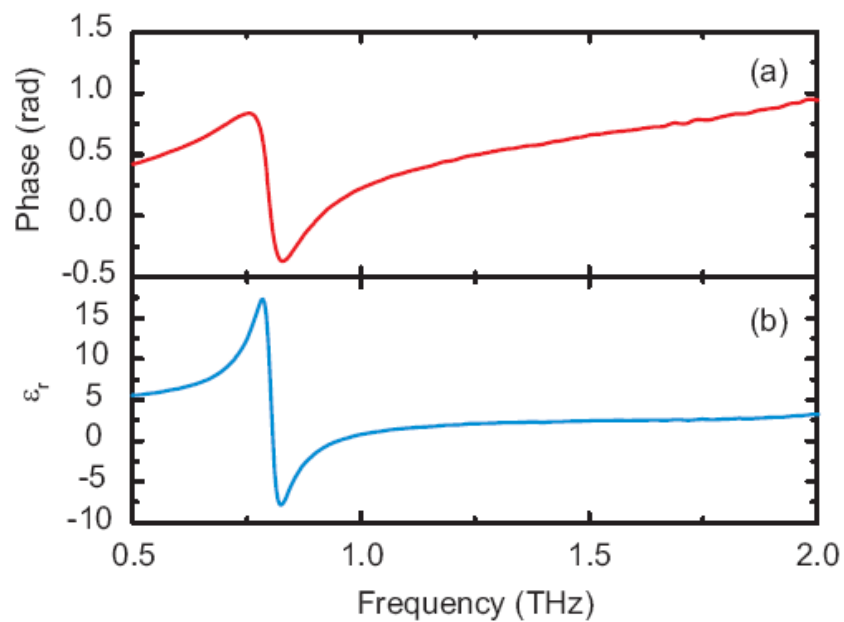


Fig. 4 (a) Phase and (b) extracted real part of the effective dielectric function of the single-layer metamaterial on 12.7- $\mu\text{m}$ -thick polyimide substrate.

Fig. 3 also reveals that even at resonance the values are positive for the real portion of the dielectric functions. This is due to the large spacing (substrate thickness) between the adjacent eSRR layers. As an effective medium, both the resonance of the metamaterial elements and the polyimide substrate contribute to the effective dielectric functions. The resonant phase perturbations shown in Fig. 2(b) are from the planar metamaterials whereas, the large phase slopes off resonance are due to the thick polyimide substrate. The super-position of these two effects leads to exclusively positive values of the effective dielectric functions over the entire bandwidth.

Decreasing the thickness of the polyimide substrates will reduce the contribution of the effective dielectric function from the substrate thereby enabling a negative electric response. This is verified by the results shown in Fig. 4 where a different SRR array [6] was fabricated on a polyimide substrate with  $12.7\mu\text{m}$  thickness. We measured the THz transmission properties of this single-layer free standing metamaterial sample (without the use of quartz plates), and the phase is shown in Fig. 4(a), which reveals negative phase delay near the resonance frequency. The corresponding effective dielectric function is extracted using  $12.7\mu\text{m}$  sample thickness, and the real portion in Fig. 4(b) shows negative values near the resonance.

#### 4. Conclusions

In conclusion, we have demonstrated quasi-three-dimensional THz metamaterials by stacking single-layer eSRR arrays fabricated on flexible, thin polyimide substrates. Using THz-TDS we measured their THz transmission properties, with which we obtained their complex effective dielectric functions. All metamaterials show a resonant response, where the transmission minimum reduces and phase dispersion increases with increasing number of layers. As effective media, the dielectric functions turn out to be largely independent on the number of layers, or the total thickness of the media. Due to the large spacing between the individual eSRR layers, near the resonance the real portions of the dielectric functions only show positive values. Negative electric response was achieved by reducing the substrate thickness and thereby its contribution to the effective dielectric function. Our results verify a fabrication approach by which quasi-bulk 3D, durable, and conformable metamaterials can be realized. These are obviously important steps in realizing functional THz metamaterial devices such as prisms, lenses, waveguides, filters, and cloaks or shields.

#### Acknowledgement

This work was performed, in part, at the Center for Integrated Nanotechnologies, a U. S. Department of Energy, Office of Basic Energy Sciences nanoscale science research center jointly operated by Los Alamos and Sandia National Laboratories. Los Alamos National Laboratory, an affirmative action equal opportunity employer, is operated by Los Alamos National Security, LLC, for the National Nuclear Security Administration of the U.S. Department of Energy under contract DE-AC52-06NA25396. We gratefully acknowledge support from the U.S. Department of Energy through the LANL/LDRD Program for this work.

## References

- [1] D. R. Smith, W. J. Padilla, D. C. Vier, S. C. Nemat-Nasser, and S. Schultz, "Composite medium with simultaneously negative permeability and permittivity," *Phys. Rev. Lett.* 84, 4184-4187, (2000).
- [2] R. A. Shelby, D. R. Smith, and S. Schultz, "Experimental verification of a negative index of refraction," *Science* 292, 77-79, (2001).
- [3] J. B. Pendry, "Negative refraction makes a perfect lens," *Phys. Rev. Lett.* 85, 3966-3969, (2000).
- [4] N. Fang, H. Lee, C. Sun, and X. Zhang, "Sub-diffraction-limit optical imaging with a silver superlens," *Science* 308, 534-537, (2005).
- [5] D. Schurig, J. J. Mock, B. J. Justice, S. A. Cummer, J. B. Pendry, A. F. Starr, and D. R. Smith, "Metamaterial electromagnetic cloak at microwave frequencies," *Science* 314, 977-980, (2006).
- [6] A. K. Azad, J. Dai, and Weili Zhang, "Transmission properties of terahertz pulses through subwavelength double split-ring resonators," *Opt. Lett.* 31, 634-634, (2006).
- [7] H.-T. Chen, J. F. O'Hara, A. J. Taylor, R. D. Averitt, C. Highstrete, M. Lee, and W. J. Padilla, "Complementary planar terahertz metamaterials," *Opt. Express* 15, 1084-1095, (2007).
- [8] T. J. Yen, W. J. Padilla, N. Fang, D. C. Vier, D. R. Smith, J. B. Pendry, D. N. Basov, X. Zhang, "Terahertz magnetic response from artificial materials," *Science* 303, 1494-1496, (2004).
- [9] T. Driscoll, G. O. Andreev, D. N. Basov, S. Palit, T. Ren, J. Mock, S. Y. Cho, N. M. Jokerst, and D. R. Smith, "Quantitative investigation of a terahertz artificial magnetic resonance using oblique angle spectroscopy," *Appl. Phys. Lett.* 90, 092508, (2007).
- [10] W. J. Padilla, A. J. Taylor, C. Highstrete, M. Lee, and R. D. Averitt, "Dynamical electric and magnetic metamaterial response at terahertz frequencies," *Phys. Rev. Lett.* 96, 107401, (2006).
- [11] H.-T. Chen, W. J. Padilla, J. M. O. Zide, A. C. Gossard, A. J. Taylor, and R. D. Averitt, "Active terahertz metamaterial devices," *Nature* 444, 597-600, (2006).
- [12] H.-T. Chen, W. J. Padilla, J. M. O. Zide, S. R. Bank, A. C. Gossard, A. J. Taylor, and R. D. Averitt, "Ultrafast optical switching of terahertz metamaterials fabricated on ErAs/GaAs nanoisland superlattices," *Opt. Lett.* 32, 1620-1622, (2007).
- [13] H.-T. Chen, J. F. O'Hara, A. K. Azad, A. J. Taylor, R. D. Averitt, D. B. Shreken-hamer, and W. J. Padilla, "Experimental demonstration of frequency-agile terahertz metamaterials," *Nature Photon.* 2, 295-298, (2008).
- [14] J. B. Pendry, A. J. Holden, D. J. Robbins, and W. J. Stewart, "Magnetism from conductors and enhanced nonlinear phenomena," *IEEE Trans. Microwave Theory Tech.* 47, 2075-2084, (1999).
- [15] J. B. Pendry, A. J. Holden, W. J. Stewart, and I. Youngs, "Extremely low frequency plasmons in metallic mesostructures," *Phys. Rev. Lett.* 76, 4773-4776, (1996).
- [16] M. Gokkavas, K. Guven, I. Bulu, K. Aydin, R. S. Penciu, M. Kafesaki, C. M. Soukoulis, and E. Ozbay, "Experimental demonstration of a left-handed metamaterial operating at 100 GHz," *Phys. Rev. B* 73, 193103, (2006).

- [17] B. D. F. Casse, H. O. Moser, J. W. Lee, M. Bahou, S. Inglis, and L. K. Jian, "Towards three-dimensional and multilayer rod-split-ring metamaterial structures by means of deep x-ray lithography," *Appl. Phys. Lett.* 90, 254106, (2007).
- [18] S. Gupta, G. Tuttle, M. Sigalas, and K.-M. Ho, "Infrared filters using metallic photonic band gap structures on flexible substrates," *Appl. Phys. Lett.* 71, 2412-2414, (1997).
- [19] N. Katsarakis, G. Konstantinidis, A. Kostopoulos, R. S. Penciu, T. F. Gundogdu, M. Kafesaki, E. N. Economou, Th. Koschny, and C. M. Soukoulis, "Magnetic response of split-ring resonators in the far-infrared frequency regime," *Opt. Lett.* 30, 1348-1350, (2005).
- [20] N. Liu, H. Guo, L. Fu, S. Kaiser, H. Schweizer, and H. Giessen, "Three-dimensional photonic metamaterials at optical frequencies," *Nature Mat.* 7, 31-35, (2007).
- [21] O. Paul, C. Imhof, B. Reinhard, R. Zengerle, and R. Beigang, "Negative index bulk metamaterial at terahertz frequencies," *Opt. Express* 16, 6736-6744, (2008).
- [22] C. P. Wong, "*Polymers for Electronic and Photonic Application*," Academic, London, p. 661, (1992).
- [23] J. F. O'Hara, J. M. O. Zide, A. C. Gossard, A. J. Taylor, and R. D. Averitt, "Enhanced terahertz detection via ErAs:GaAs nanoisland superlattices," *Appl. Phys. Lett.* 88, 251119, (2006).
- [24] W. Zhang, A. K. Azad, and D. Grischkowsky, "Terahertz studies of carrier dynamics and dielectric response of n-type, freestanding epitaxial GaN," *Appl. Phys. Lett.* 82, 2841-2843, (2003).
- [25] D. R. Smith, S. Schultz, P. Markos, and C. M. Soukoulis, "Determination of effective permittivity and permeability of metamaterials from reflection and transmission coefficients," *Phys. Rev. B* 65, 195104, (2002).
- [26] D. Schurig, J. J. Mock, and D. R. Smith, "Electric-field-coupled resonators for negative permittivity metamaterials," *Appl. Phys. Lett.* 88, 041109, (2006).